High-spin octupole yrast levels in $^{216}Rn_{86}$

M. E. Debray,[1,2,*] J. Davidson,[3] M. Davidson,[3] A. J. Kreiner,[1,2,3] M. A. Cardona,[1,2,3] D. Hojman,[1,3] D. R. Napoli,[4] S. Lenzi,[5] G. de Angelis,[4] D. Bazzacco,[5] S. Lunardi,[5] M. De Poli,[4] C. Rossi-Alvarez,[5] A. Gadea,[4] N. Medina,[6] and C. A. Ur[5]

[1]*Departamento de Física, Comisión Nacional de Energía Atómica, 1429 Buenos Aires, Argentina*

[2]*Escuela de Ciencia y Tecnología, Universidad de San Martín, Argentina*

[3]*CONICET, 1033 Buenos Aires, Argentina*

[4]*INFN, Laboratori Nazionali di Legnaro, Legnaro, Italy*

[5]*Dipartimento di Fisica, Sezione di Padova, Padova, Italy*

[6]*Departamento de Fisica Nuclear, Universidade de Saõ Paulo, Brazil*

(Received 10 November 2005; published 17 February 2006)

The yrast level structure of ^{216}Rn has been studied using in-beam spectroscopy α-γ-γ coincidence techniques through the ^{208}Pb(^{18}O, $2\alpha 2n$) reaction in the 91–93 MeV energy range, using the 8π GASP-ISIS spectrometer at Legnaro. The level scheme of ^{216}Rn resulting from this study shows alternating parity bands only above a certain excitation energy. From this result, the lightest nucleus showing evidence of octupole collectivity at low spins is still ^{216}Fr, thereby defining the lowest-mass corner for this kind of phenomenon as $N \geqslant 129$ and $Z \geqslant 87$.

DOI: 10.1103/PhysRevC.73.024314 PACS number(s): 21.10.Re, 23.20.Lv, 25.70.Gh, 27.80.+w

I. INTRODUCTION

^{216}Rn has four protons and four neutrons more than the doubly closed-shell nucleus ^{208}Pb, and it lies at the edge of the transitional region of the nuclidic chart in which octupole collectivity starts to appear. The low-lying level scheme of ^{216}Rn has been previously studied up to $J^{\pi} = 10^{+}$ through the ^{208}Pb(^{14}C, $\alpha 2n$)^{216}Rn reaction [1]. In that study, the proposed level scheme did not exhibit at low spins the alternating parity structure observed in its heavier neighbors [2–6]. The lightest nucleus known to date showing evidence of octupole collectivity near the ground state is the odd-odd isotope ^{216}Fr [2]. In fact, the transition between the spherical shell model and a collective regime seems to occur at $N = 129$ and $Z = 87$. The nucleus ^{216}Rn [1] shows evidence of the development of some quadrupole collectivity, but no low-lying negative parity states are observed. On the other hand, the Fr isotopes are located at the edge ($Z = 87$ in number of protons) of the region for which octupole collectivity starts. The known odd-Z and doubly odd nuclei in this transitional region ($N \geqslant 129$, $Z \geqslant 87$), which show quadrupole and octupole collectivity, generally display weak coupling-type schemes, in which the unpaired proton couples to collective states in the neighbors, largely preserving their structure. This is true for ^{216}Fr [2] and ^{218}Ac [3,4] in which the removal or addition of the odd $h_{9/2}$ proton does not influence significantly the structure already developed in ^{217}Ra [5]. The nearest heavier isotone ^{217}Fr [6] shows quite regular low-spin alternating parity bands. The purpose of this study is to compare the level structure of ^{216}Rn and its known isotone and isotopes and provide additional information that hopefully will contribute to understanding the onset of octupole collectivity in the light actinide region.

*Electronic address: debray@tandar.cnea.gov.ar

II. EXPERIMENTAL PROCEDURES

The nucleus ^{216}Rn has been studied through the ^{208}Pb(^{18}O, $2\alpha 2n$) reaction at 91 and 93 MeV bombarding energies using the 8π GASP-ISIS spectrometer at Legnaro. A 2 mg/cm^2 self-supporting ^{208}Pb target was bombarded with a 10 nA ^{18}O beam. The spectroscopy of nuclei in this mass region is hampered by the very small incomplete fusion cross sections [7] (in the reactions used, of only a few tens of μb) and the intense background originated from fission. To reduce this intense γ background, we used the ISIS array (40 telescopic E-ΔE particle detectors) to trigger the GASP spectrometer, selecting the α particles emitted in coincidence with transitions between excited states in ^{216}Rn. This powerful technique and the transitions known from previous work [1] were used here to identify unambiguously the γ transitions belonging to this nucleus. At the bombarding energies used in the present reaction, the cross section for the $2\alpha 2n$ channel was estimated to be $\sigma \simeq 40\,\mu$b.

The predominant transitions were assigned to ^{216}Rn from the coincidence with 2α particles firing one or two ΔE detectors of the ISIS array, in which the separation between the α's belonging to the $2\alpha 2n$ channel and the charged particles arising from other reaction channels was very clear [7]. Only a very small contamination from the $\alpha 3n$ channel (^{219}Ra [8]) was present. A total of some 300,000 events were acquired from the γ-γ-ΔE coincidences ($2\alpha xn$ channels, 2/3 of them corresponding to ^{216}Rn).

A positive identification of the γ rays belonging to Z = 86 nuclei was based on the coincidence between Rn K x rays and the most intense lines present in the projection spectrum. This is the γ-ray spectrum in coincidence with 2α hits in the ISIS array, two in the BGO multiplicity filter, and two in the Ge detectors (see Fig. 1).

The isotopic assignment of lines belonging to ^{216}Rn was based on the reaction energy and prior knowledge of a few transitions from previous work [1].

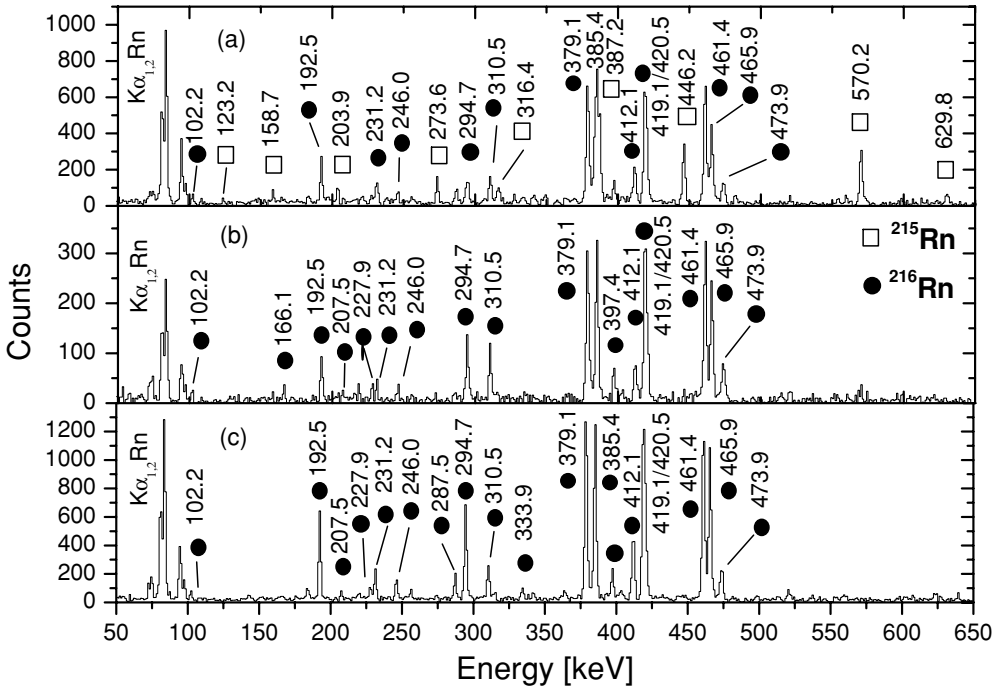

FIG. 1. γ-ray coincidence spectra of Ge detectors (γ-γ coincidence with $2\alpha'$s in one or two ΔE detectors of the ISIS array) corresponding to (a) gate on $K_{\alpha,\beta}$ Rn x rays, (b) sum of coincidence spectra gated on the more intense quadrupole and dipole transitions above the $J^{\pi} = 12^{+}$ state (see Fig. 2), and (c) sum of coincidence gates on the 461.4, 379.1, 385.4, and 419.1 keV transitions.

In order to determine the multipolarities for the γ transitions, (DCO) ratios were obtained. Due to low statistics of the data, only the anisotropy ratios R defined as the intensity ratio of transitions observed in the 32°/148° detector rings to those detected in the 90° ring, were extracted. The assignments were consistently checked with transitions of known multipolarity belonging to ^{219}Ra and ^{216}Rn. In addition, extensive use was made of coincidence intensity balance. In particular, the $E1$ character of the 192.7, 227.9, and 246.0 keV transitions follows from a careful consideration of the intensity balance in coincidence spectra gated above each line in question. $M1$ character for these transitions is ruled out by these intensity balances because of the large internal conversion coefficients associated with this multipolarity. The $E1$ character for the 166.1, 207.5, and 231.2 keV transitions, which is consistent with the coincidence intensity data, follows from their placement into the level scheme (see next section).

III. THE LEVEL SCHEME

The γ rays assigned to ^{216}Rn are listed in Table I together with their relative intensities and the anisotropy values. The assigned multipolarities were adopted by means of intensity balance and anisotropy ratios. A very powerful aid in the construction of the level scheme was the cleanliness of the projection spectrum (see Fig. 1). Only a few transitions belonging to ^{216}Rn are slightly contaminated with ^{219}Ra [8] transitions. This situation allows an intensity determination for the majority of the ^{216}Rn transitions. The level scheme of ^{216}Rn deduced from the present study is shown in Fig. 2. The transitions observed in the previous work by Cottle *et al.* [1] up to the 1645 keV state ($J^{\pi} = 8^{+}$) were confirmed. The lower position of the 461.4, 379.1, 385.4, and 419.1 keV cascade in the level scheme is strongly supported by the coincidence with the 287.0, 410.5, and 622.9 keV transitions. Furthermore, in spite of the fact that an intensity balance does not allow one to unambiguously establish the relative position of the 379.1 and 385.4 keV transitions, the location of the 419.1 keV transition is unequivocally established by the presence of the 559.8 keV transition.

The prior [1] relative position of the 465.9 keV transition in the level scheme was altered, and the 294.7 keV transition, which was previously assigned [1] as a ^{219}Ra contamination, is, according to our data, an important transition of ^{216}Rn which appears clearly in coincidence with the strong low-lying cascade: 461.4, 379.1, 385.4, and 419.1 keV transitions.

The present ordering of the 465.7 and 294.7 keV transitions was determined from a careful intensity balance on sum gates on the 461.4, 379.1, and 385.4 keV transitions and on the 192.7/192.5, 420.5 keV, and 473.9 keV gates. The anisotropy ratio for the 294.7 keV line seems to support its quadrupolar character. The 294.7 keV transition is assumed to have a stretched $E2$ character as a result of a careful intensity balance for different gates taking into account all possible multipolarity ($E2$, $M1$, $E1$) combinations for the 102.2 and 192.5 keV transitions. These intensity balances are compatible (within errors) only with $E2$ (multipolarity) for both transitions. Nevertheless, from these intensity balances it is not possible to determine the relative order of the 102.2 and 192.5 keV transitions.

TABLE I. γ-ray energies, intensities, anisotropy ratios (defined as the intensity ratio of transitions observed in the 32°/148° detector rings to those detected in the 90° ring of the GASP spectrometer) and adopted multipolarities. Data correspond to the ^{208}Pb(^{18}O, $2\alpha 2n$) reaction in the 91–93 MeV energy range.

E_γ^a (MeV)	I_γ	R^*	I^{Tot}	Adopt.[b] mult.
102.2[c]	2.4(4)		32(6)	$(E2)$[d]
166.1	2.7(4)		2.9(4)	$E1$[e]
185.6	$\leqslant 1$			
192.5[c]	9.2(1.6)	0.60(0.10)	28(5)	$(E2)$[d]
192.7[c]	25.6(3.8)		27(4)	$E1$[d]
207.5[c]	4.1(0.9)	0.70(0.11)	4.2(1.0)	$E1$[e]
227.9	7.8(0.9)		8.0(1.4)	$E1$[d]
231.2	15.8(1.1)	0.59(0.10)	16.1(2.5)	$E1$[e]
246.0	11.7(1.0)	0.69(0.11)	11.8(1.0)	$E1$[d]
287.0[f]	7.0(2.0)			
292.7	6.0(1.2)		6.1(1.5)	
294.7[c]	43.1(3.6)	1.16(0.26)	47.4(4.0)	$E2$[d]
310.5[c]	23.3(3.0)	1.26(0.22)	25.2(3.2)	$E2$
333.9[c]	7.0(1.4)		7.4(1.5)	$E2$[d]
379.1[c]	96.8(4.2)	1.04(0.16)	98.4(4.3)	$E2$
385.4	95.4(6.1)	1.13(0.21)	96.7(6.3)	$E2$
397.4	17.0(2.1)	1.18(0.17)	17.3(2.2)	$E2$
410.5[f]	6.0(2.0)			
412.1[c]	36.6(3.0)	1.12(0.16)	37.1(3.0)	$E2$
419.1[c]	94.5(6.4)	1.18(0.20)	97.9(6.5)	$E2$
420.5[c]	42.4(5.1)	1.16(0.23)	42.9(5.2)	$E2$
461.4	100.0(4.0)	1.12(0.16)	100.0(4.0)	$E2$
465.9	70.4(3.6)	1.26(0.23)	70.4(3.6)	$E2$
473.9	16.3(2.1)		17.0(2.2)	$E2$
498.9	4.3(0.8)		4.3(0.8)	$(E2)$
520.5	9.6(1.9)		9.6(1.5)	
559.8[f]	3.0(1.0)			
622.9[f]	3.0(1.0)			

[a]Errors in E_γ are about 0.2 keV.

[b]Multipolarities in parenthesis are propositions which are not confirmed.

[c]Contaminated lines. Relative intensities were deduced from coincidence spectra.

[d]The electric or magnetic character is deduced from total intensity balance in coincidence spectra.

[e]The $E1$ character, consistent with the coincidence intensity data, follows from the placement into the level scheme.

[f]Are in coincidence with the most intense transitions of ^{216}Rn. The multipolarities were not determined.

Figure 1(b) shows the sum of coincidence spectra gated on the quadrupole and dipole transitions above the $J^\pi = 12^+$ state; and Fig. 1(c), the sum of coincidence gates on the 461.4, 379.1, 385.4, and 419.1 keV transitions. Several new transitions (shown in Fig. 1) and a band structure with interleaved states of alternating parity connected by $E1$ transitions were found above the 2405.6 keV state. The $E2$ character of the 420.5, 412.1, 397.4, and 310.5 keV transitions and the $E1$ multipolarity of the 192.7, 227.9, and 246.0 keV transitions were determined from the anisotropy ratios and intensity balance in coincidence spectra (see previous section and Table I). These facts establish the opposite parity sequences: 12^+, 14^+, 16^+, and 13^-, 15^-, 17^-, 19^-. Hence, we are led to a level scheme showing a high-spin alternating parity band structure characteristic of octupole collectivity.

IV. DISCUSSION

The known even $N = 128$ isotones ^{214}Rn [9,10], ^{216}Ra [11], and ^{218}Th [12] have $R_4 (= E_{4^+}/E_{2^+})$ ratios less than the critical value 1.82 in the Mallmann plot [13–16] showing compression of the transition energies with increasing angular momentum of the ground state band and the existence of an isomer at spin 8^+. This common feature can be well understood within the context of the spherical shell model, with two neutrons in the $g_{9/2}$ and the valence protons coupled to zero. On the other hand, the known $N = 130$ isotones ^{218}Ra [17,18] and ^{220}Th [12] show undoubtedly collective characteristics, and their R_4 ratios lie beyond $R_4 = 1.82$ (1.90 and 2.03, respectively). Furthermore, the odd isotones ^{217}Fr [6] and ^{219}Ac [19] can be described as the weak coupling of an $h_{9/2}$ proton hole and an $h_{9/2}$ proton to the ^{218}Ra core, respectively. Nevertheless, the energy at which the octupole excitation starts, decreases with increasing proton number (1355 keV for ^{217}Fr, 793 keV for ^{218}Ra, and 657.6 keV for ^{219}Ac). It is noteworthy that in ^{216}Rn, the R_4 ratio coincides with the critical 1.82 value (see discussion in Ref. [2]).

The nucleus ^{216}Rn shows only at higher excitation energies an alternating parity pattern similar to the one of its heavier isotones, but it also displays features reminiscent of a spherical shell model. That is the case of the 1939.7 keV state. Because of the features present in the ^{216}Rn level scheme, it is convenient to divide the discussion in three parts:

(i) The low-lying level band up to the 1645.0 keV state
(ii) The 1939.7 keV, 10^+ state
(iii) The structure on top of the 1939.7 keV state

(a) This part of the level scheme shows a rather regular positive parity ground state band with a weak initial compression of the transition energies with increasing angular momentum. The $R_4 = 1.82$ value (see Refs. [2,14–16]) is an indication of the onset of collective features. At the $I^\pi = 8^+$ state, the level scheme shows a pronounced modification of this regularity.

(b) This 10^+ state may be understood, in the $N = 130$ isotones, as the coupling of four protons and four neutrons to the $[\pi h_{9/2}^4(0) \otimes (\nu g_{9/2}^2)(0) \otimes (\nu g_{9/2} \otimes \nu i_{11/2})(10)]$ dominant configuration (using a simplified nomenclature $[h^4(0)][g^2(0)][gi(10)]$). Such a low-seniority state has been found in the nearest lighter isotope ^{214}Rn [10] in which the 10^+ state at 1928 keV excitation energy has predominantly seniority two, with the four protons coupled to zero. The state at 1837.5 keV is likely to be associated to the $[h^4(0)][g^2(0)gi(8,9)]$ predominant configuration. [From a purely experimental point of view, the allowed spin-parity values are $(8, 9, 10)^+$]. Since $g_{9/2}$ and $i_{11/2}$ are orbitals near the Fermi surface, their quasiparticle character may imply a quenching of the $[g_{9/2} \otimes i_{11/2}](J)$ multiplet [14].

Figure 3 shows the one-quasiparticle energies for neutrons (a) and protons (b) vs the number of protons (neutrons) above the $N = 126$, $Z = 82$ doubly magic gap, relative to the ground state of their respective nuclei. From this information,

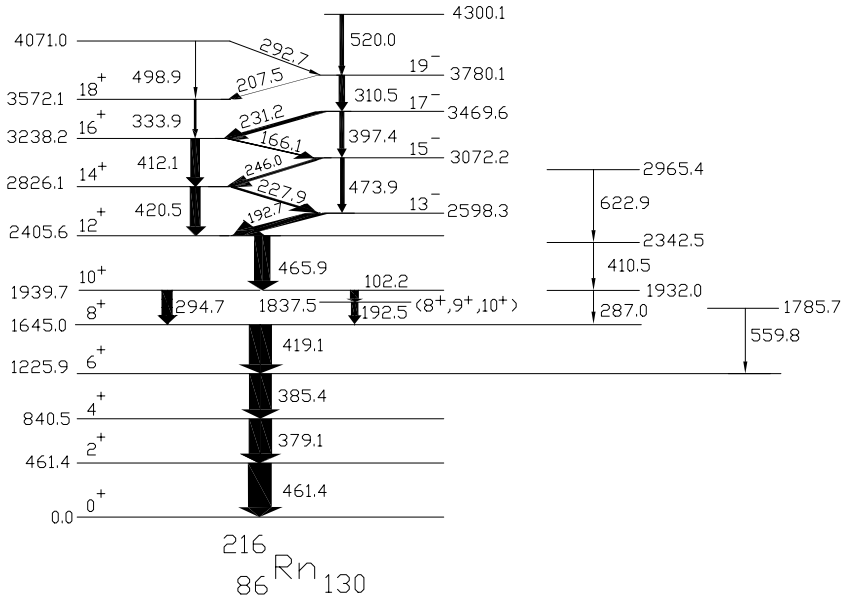

FIG. 2. Experimental level scheme of ^{216}Rn proposed in the present work. The relative arrow widths indicate the total transition intensities and correspond to the ^{208}Pb(^{18}O, $2\alpha 2n$) reaction in the 91–93 MeV energy range.

it is possible to estimate the zero-order excitation energy of the $[h^4(0)][g^2(0)][gi(10)]$ state at 1939.7 keV in ^{216}Rn. The 294.7 keV excitation energy above the $I^\pi = 8^+$ at 1645.0 keV corresponds approximately to an energy value intermediate between the $\nu i_{11/2}$ one-quasiparticle energies of ^{215}Rn (316.4 keV) [20] and ^{217}Rn (89.1 keV) [21]; while according to the nearly equidistant energies of the ground state band, the $I^\pi = 10^+$ which would arise from the addition of one quadrupolar phonon on top of the $I^\pi = 8^+$ state should be found (if it exists) at an excitation energy (the average transition energy of the ground state band is approximately 411 keV higher than 1939.7 keV), and therefore it is not expected to be observed since it will not be an yrast state.

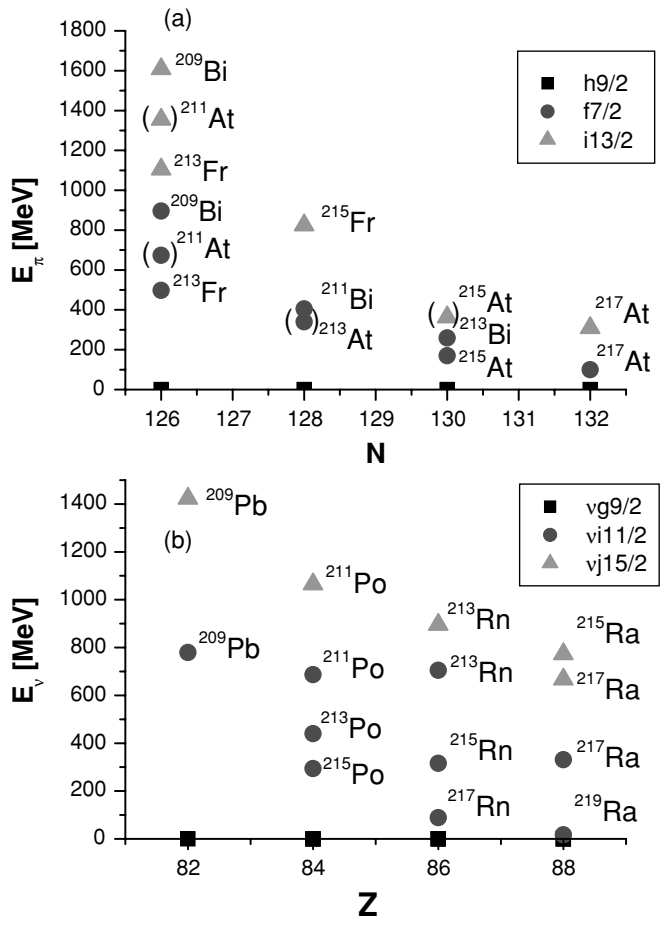

FIG. 3. Single-particle energy evolution for neutrons (a) and protons (b) beyond the closed shell $N = 126$.

(c) The cascade beginning with the 465.9 keV transition shows two band structures with interleaved states of alternating parity connected by enhanced $B(E1)$ transitions. Experimental $B(E1)/B(E2)$ ratios for ^{216}Rn (shown in Table II) were obtained for each excited state by measuring the $E1/E2$ γ-ray intensity ratio from a spectrum which was in coincidence with all the transitions lying above the state of interest. The $B(E1)/B(E2)$ ratio for the transitions $19^- \longrightarrow 18^+$ and $19^- \longrightarrow 17^-$ is an order of magnitude smaller than the $B(E1)/B(E2)$ ratios observed for the transitions from negative to positive parity states up to the 17^- state. Values as small as this reduced value have also been observed in the heavier isotopes ^{218,220}Rn [22].

The average value $\overline{B(E1)/B(E2)} = 3.2 \times 10^{-7}$ fm^{-2} found in ^{216}Rn, turns out to be 7.4 times smaller than the average value for ^{218}Ra, 2.3×10^{-6} fm^{-2} [23] and 5.6 times

TABLE II. $B(E1)/B(E2)$ ratios in ^{216}Rn (this work), ^{218}Ra [23], and ^{220}Th [12] for states of the same spin.

^{216}Rn		^{218}Ra		^{220}Th	
I_i^π	$B(E1)/B(E2)$ (10^{-6} fm^{-2})	I_i^π	$B(E1)/B(E2)$ (10^{-6} fm^{-2})	I_i^π	$B(E1)/B(E2)$ (10^{-6} fm^{-2})
(14^+)	0.16(3)	14^+	1.2(4)	14^+	1.8(4)
(15^-)	0.7(1)	15^-	1.4(3)	15^-	2.8(7)
(16^+)	0.13(3)	16^+	0.8(3)		
(17^-)	0.6(1)				
(19^-)	0.05(2)				

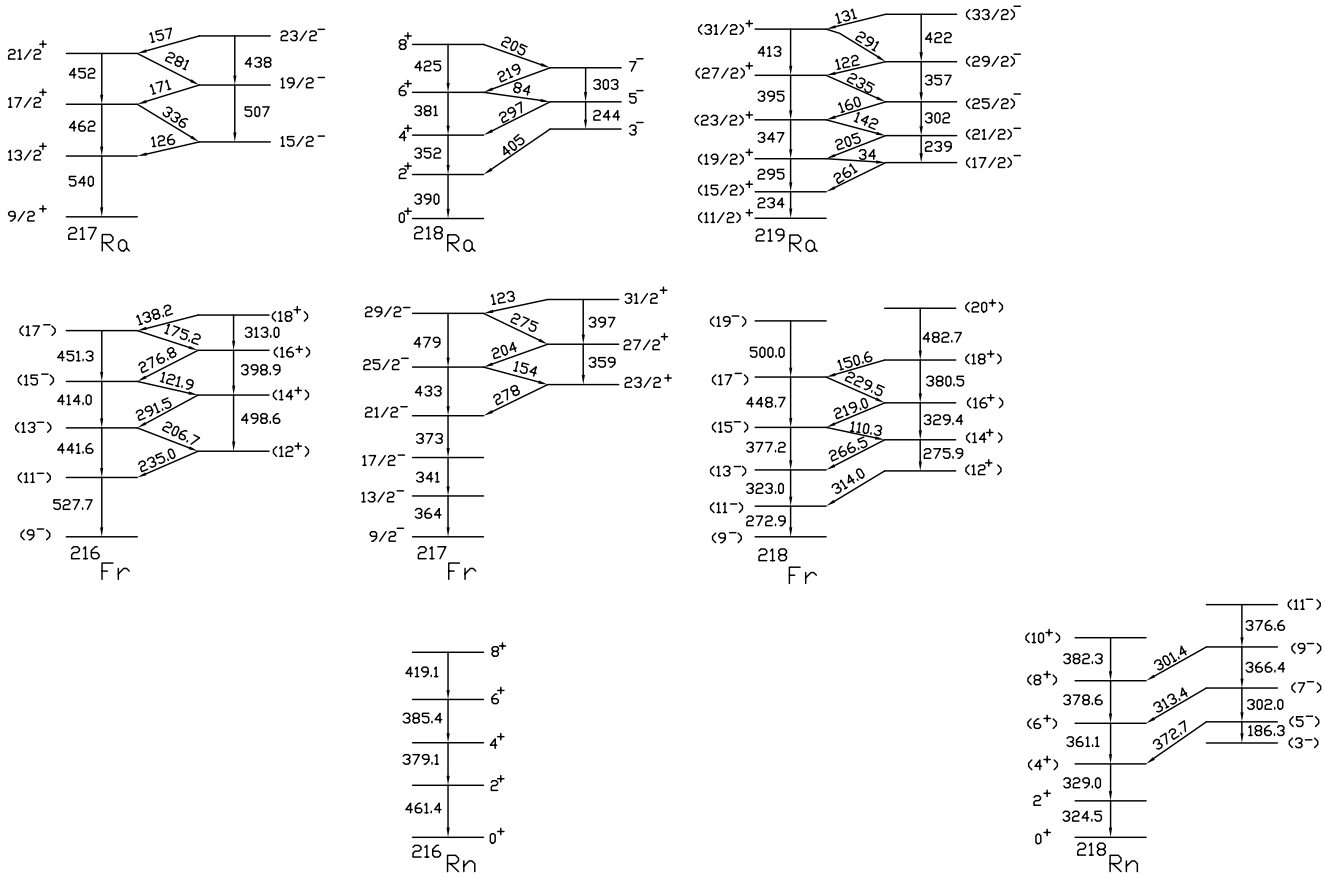

FIG. 4. Comparison of the low-lying level schemes of the light actinide isotones Rn, Fr, and Ra ($129 \leqslant N \leqslant 131$ and $86 \leqslant Z \leqslant 88$). The transition between a spherical shell model and a collective regime seems to start at ($N = 129$, $Z = 87$) and ($N = 130$, $Z = 86$).

smaller than the average value for ^{220}Th, 1.8×10^{-6} fm^{-2} [12]. The $B(E1)/B(E2)$ ratios show a pronounced staggering as a function of spin (see Table II). They are larger for transitions from negative to positive parity states than for transitions from positive to negative parity states. For pure vibrations [24] (and if only s, d, and f bosons are considered), the $E1$ transitions from positive $[I^+]$ to negative $[(I-1)^-]$ states are forbidden. A similar argument holds for an octupole vibration coupled to a deformed core. For stable octupole shapes, on the other hand, these ratios should be similar for transitions starting from either positive or negative parity states. The $B(E1)/B(E2)$ ratios observed in ^{216}Rn (and for the other transitional neighbors ^{216}Fr [2], ^{217}Ra [5], and ^{218}Ac [4]) show an intermediate behavior between the two extremes just discussed.

The quasiharmonic behavior of the quadrupole transition energies with increasing angular momentum and the staggering of the $B(E1)/B(E2)$ ratios and their smaller values (see Table II) add strong points for the case of a development of quadrupolar and octupolar collectivity in the Rn isotopic chain starting at ^{216}Rn.

Absolute values of the ratio of the intrinsic dipole moment $|D_0|$ and intrinsic electric quadrupole moment $|Q_0|$ were extracted from the $B(E1)/B(E2)$ values using the experimental $E1/E2$ γ-ray intensity ratios and the rotational model formula [25]. Q_0 is assumed to remain constant over the observed spin range. In spite of the fact that the use of this expression is questionable since ^{216}Rn is not a good rotor, this is a consistent method for extracting $|D_0|$ from the data and allows us to compare our results with other quoted values for $|D_0|$ obtained in the same way. The mean value of this ratio for ^{216}Rn is $|\overline{D_0/Q_0}| = 0.28 \pm 0.07\ 10^{-3}$ fm^{-1}. As an intrinsic electric quadrupole moment has not been measured for ^{216}Rn, Grodzins' relation [26](for the $2^+ \longrightarrow 0^+$ transition) for even-even nuclei was used to estimate a Q_0 value of 301 e fm^2. Hence, the obtained "experimental" mean dipole moment $|\overline{D_0}| = 0.085 \pm 0.02e$ fm is approximately a factor of 3 or 4 lower than those of ^{218}Ra, ^{219}Ra, and ^{220}Th, a factor 2 lower than that of ^{217}Fr, and twice the values measured for ^{218}Rn and ^{220}Rn ([22,27] and refs. therein). Such small values for Rn isotopes are predicted by microscopic-macroscopic calculations [27] to be a consequence of the small deformation and the cancellation between the macroscopic and shell contributions to the intrinsic dipole moment. However, the increased experimental $|\overline{D_0}|$ value found in ^{216}Rn as compared to ^{218}Rn can be understood as due to the spin difference of the states from which the value is extracted. The first result is a mean value for $I = 14-19$, and the $|\overline{D_0}|$ values of ^{218}Rn and ^{220}Rn were measured for $I = 7$ and $I = 5-9$, respectively [22]. Also, the theoretical D_0 values for ^{218}Rn and

^{220}Rn [27] were calculated in the ground state. Soft nuclei like ^{216}Rn, which are expected to be octupole undeformed at $I = 0$, may become octupole unstable at high spins. This statement is predicted to be valid for its neighboring isotone ^{218}Ra, in which octupole deformed configurations become yrast at high spins with relatively large values of β_3 and relatively small quadrupole deformations [28]. The increase of experimental $|\overline{D_0}|$ values for the isotones with $N = 130$ may indicate that the p-n octupole correlations are larger for larger proton numbers.

It is interesting now to examine the general features of the light actinides in the neighborhood of ^{216}Rn. Figure 4 presents a systematic of this region of actinides (Rn, Fr, and Ra; $129 \leqslant N \leqslant 131$ and $86 \leqslant Z \leqslant 88$). For $N = 129$, the similarity between ^{216}Fr and ^{217}Ra suggests that the $h_{9/2}$ proton hole is only weakly coupled, because it does not influence the structure developed in ^{217}Ra [5]. In fact, the transition between the spherical shell model and the collective regime seems to start at $N = 129$. In the isotones with $N = 130$, we find a similar weak coupling picture between the level schemes of ^{217}Fr and ^{218}Ra. Besides, the R_4 ratios are very close and beyond the critical value 1.82 in the Mallmann plot [14,15] (1.90 for ^{218}Ra). On the other hand, the addition of an $h_{9/2}$ proton to ^{216}Rn alters the structure of the ground state band, and it seems to trigger the octupole collectivity, since the alternating parity band in ^{217}Fr starts at a significantly lower energy [6].

Figure 5 shows the evolution of the excitation energies for some negative parity states of the known isotopes of Ra, Th, and Rn as functions of neutron number, and Fig. 6 shows the evolution of the excitation energies for yrast states of the known isotopes of Rn as a function of neutron number. With increasing neutron number, the energy of the 2^+ ground state band decreases steeply from 324.5 in ^{218}Rn to 186.4 keV in ^{222}Rn (≈42%), while the energy of the 3^- state decreases only ≈24% from ^{218}Rn (839.9) to ^{222}Rn (635.0 keV). These

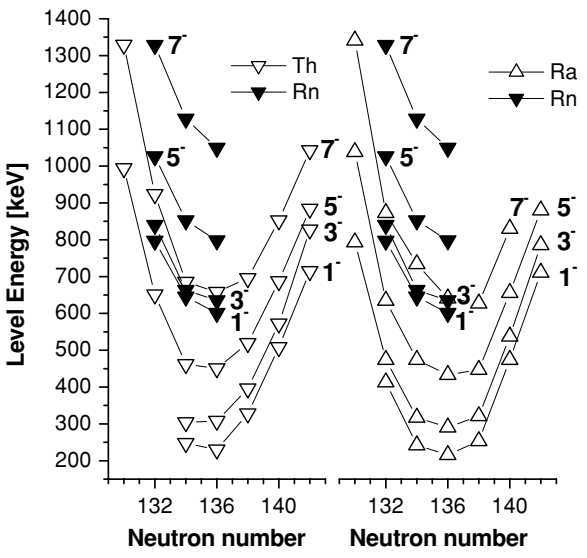

FIG. 5. Low-lying negative parity yrast level systematic of the even-even Th, Ra, and Rn isotopes. Empty symbols are data from Refs. [5] and [22]; full symbols are data obtained in this work.

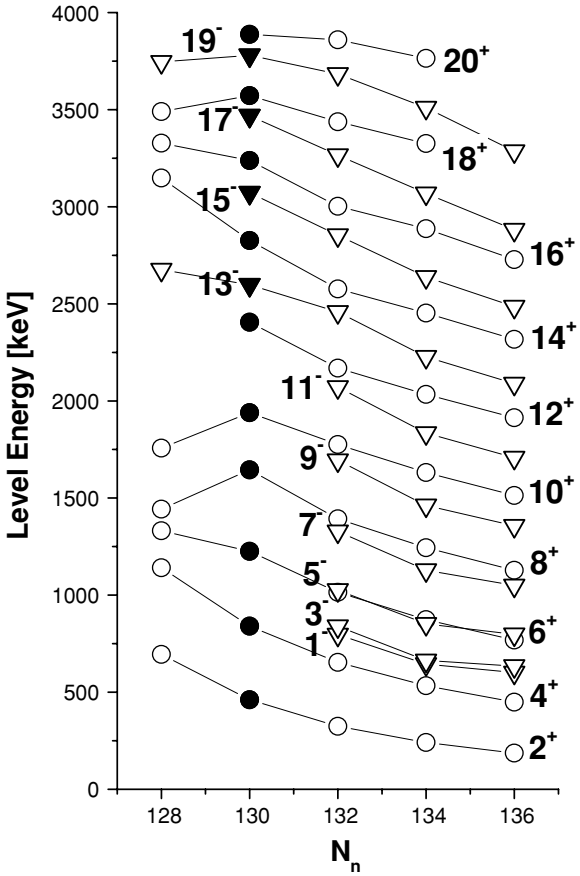

FIG. 6. Yrast level systematics for excited states of Rn isotopes as function of neutron number. Inverted triangles correspond to odd spin states, and circles to even spin states. Empty symbols are data from Ref. [22] (^{218,220,222}Rn) and Ref. [10] (^{214}Rn), full symbols are data obtained in this work.

changes are more important in the Ra isotopes, in which the energy of the 2^+ state decreases from 178.5 in ^{218}Ra (isotone of ^{216}Rn) to 84.5 keV in ^{224}Ra (isotone of ^{222}Rn) (≈53%), while the energy of the 3^- state decreases for the same nucleus from 474.2 to 290.4 keV (≈39%).

In fact, the nucleus ^{222}Rn has moved a long way towards a deformed situation as compared to ^{216}Rn as far as the quadrupole degree of freedom is concerned (but not so much for the octupole collectivity). The Rn isotopes appear to be octupole vibrational in nature with a rapid alignment of the octupole phonon with the rotational axis as excitation energy increases (see Ref. [22] and discussion therein).

The first confirmed negative parity state in ^{216}Rn appears at an excitation energy of 2598.3 keV and an angular momentum of $I^\pi = 13^-$. These values are significantly higher than the values observed for the negative parity states in its heavier isotones, namely 0.794 MeV and $I^\pi = 3^-$ for ^{218}Ra and 0.994 MeV and $I^\pi = 5^-$ for ^{220}Th. In fact, this is valid for all the known transitional nuclei of this region which present alternating parity bands at 0.763, 1.356, and 0.587 MeV for ^{216,217,218}Fr [2,6,29], 0.666 and 0.495 MeV for ^{217,219}Ra [5,8], and 0.667 and 0.965 MeV for ^{218,219}Ac [4,19]. Despite this result, the excited energies of ^{216}Rn fit well into the low-lying

yrast level systematics of the radon nuclei. From Fig. 5 one can see that up to $N = 136$, the positive and negative parity states show a similar trend. It is a well known fact that the steady decrease in the even and odd spin state excitation energies with increasing neutron number is related to an increase in the quadrupolar and octupolar (up to $N \simeq 134$ or 136, see Refs. [4,12]) collectivity. It follows from this systematics, that the quadrupolar and octupolar degrees of freedom appear simultaneously at low spin states for $N = 132$. The smoothness of the curves may allow the extrapolation of the 11^- curve. The 12^+ seems to cross the 11^- curve for $N \leqslant 132$ (below this neutron number, the 11^- curve is higher in energy than the 12^+ curve). At $N = 130$, the $I^\pi = 11^-$ state should be found above or very close to the $I^\pi = 12^+$ state. At spins lower than 13^-, the negative parity band has lost its yrast character. This fact may explain the high spin start of the negative parity states in the experimental level scheme.

$A = 216$ may be taken as the lower limit for the starting of octupole collectivity in nuclei with $Z = 86$.

V. CONCLUSIONS

In summary, high spin states in ^{216}Rn were populated using the ^{208}Pb(^{18}O, $2\alpha 2n$) reaction and the 8π GASP-ISIS spectrometer at Legnaro. In order to make clean spectroscopy and resolve the transitions of interest from the intense fission γ background, we trigger the γ detectors of the GASP spectrometer with the E-ΔE particle detectors of the ISIS array, selecting the evaporation α particles emitted in coincidence with transitions between excited states in ^{216}Rn. A significantly enlarged level scheme showing interleaved bands of alternating parity has been observed, but only above spin 13^-. The staggering of the $B(E1)/B(E2)$ ratios and the small (effective) $|\overline{D_0}|$ values found in ^{216}Rn are consistent with an octupole vibrational-like interpretation of this nucleus. Some features may be more naturally framed into a vibrational language, while others may be described in a particle picture. All these characteristics show that ^{216}Rn is clearly a transitional nucleus, indicating a lower mass limit ($Z = 86$, $N \leqslant 130$) for the region in which the development of the octupole collectivity starts.

[1] P. D. Cottle, M. Gai, J. F. Ennis, J. F. Shriner Jr., S. M. Sterbenz, D. A. Bromley, C. W. Beausang, L. Hildingsson, W. F. Piel Jr., D. B. Fossan, J. W. Olness, and E. K. Warburton, Phys. Rev. C **35**, 1939 (1987).

[2] M. E. Debray, J. Davidson, M. Davidson, A. J. Kreiner, D. Hojman, D. Santos, K. Ahn, D. B. Fossan, Y. Liang, R. Ma, E. S. Paul, W. F. Piel, and N. Xu, Phys. Rev. C **41**, R1895 (1990).

[3] M. E. Debray, M. Davidson, A. J. Kreiner, J. Davidson, G. Falcone, D. Hojman, and D. Santos, Phys. Rev. C **39**, R1193 (1989).

[4] M. Debray, A. J. Kreiner, M. Davidson, J. Davidson, D. Hojman, D. Santos, V. R. Vanin, N. Schulz, A. Chevallier, and J. Chevallier, Nucl. Phys. **A568**, 141 (1994).

[5] N. Roy, D. J. Decman, H. Kluge, K. H. Maier, A. Maj, C. Mittag, J. Fernández Niello, H. Puchta, and F. Riess, Nucl. Phys. **A426**, 379 (1984).

[6] M. Aïche, A. Chevallier, J. Chevallier, S. Hulne, S. Khazrouni, N. Schulz, and J. C. Sens, J. Phys. G **14**, 1191 (1988).

[7] D. Hojman *et al*., to be published.

[8] P. D. Cottle, M. Gai, J. F. Ennis, J. F. Shriner Jr., D. A. Bromley, C. W. Beausang, L. Hildingsson, W. F. Piel Jr., D. B. Fossan, J. W. Olness, and E. K. Warburton, Phys. Rev. C **33**, R1855 (1986); **36** 2286 (1987).

[9] T. Lönnroth, D. Horn, C. Baktash, C. J. Lister, and G. R. Young, Phys. Rev. C **27**, 180 (1983).

[10] G. D. Dracoulis, A. P. Byrne, A. E. Stuchbery, R. A. Bark, and A. R. Poletti, Nucl. Phys. **A467**, 305 (1987).

[11] A. Chevallier, J. Chevallier, B. Haas, S. Khazrouni, and N. Schulz, Z. Phys. A **308**, 277 (1982).

[12] W. Bonin, H. Backe, M. Dahlinger, S. Glienke, D. Habs, E. Hanelt, E. Kankeleit, and B. Schwartz, Z. Phys. A **322**, 59 (1985).

[13] M. A. J. Mariscotti, Phys. Rev. Lett. **24**, 1242 (1970).

[14] A. J. Kreiner, Phys. Rev. C **22**, 2570 (1980).

[15] A. J. Kreiner, Phys. Rev. C **30**, 371 (1984).

[16] A. J. Kreiner and C. Pomar, Phys. Rev. C **36**, 463 (1987).

[17] J. Fernández Niello, H. Putcha, F. Riess, and W. Trautmann, Nucl. Phys. **A391**, 221 (1982).

[18] M. Gai, J. F. Ennis, M. Ruscev, E. C. Schloemer, B. Shivakumar, S. M. Sterbenz, N. Tsoupas, and D. A. Bromley, Phys. Rev. Lett. **51**, 646 (1983).

[19] M. W. Drigert and J. A. Cizewski, Phys. Rev. C **31**, R1977 (1985).

[20] R. K. Sheline, C. F. Liang, P. Paris, A. Gizon, and V. Barci, Phys. Rev. C **49**, 725 (1994).

[21] M. E. Debray *et al*., to be published.

[22] J. F. C. Cocks, D. Hawcroft, N. Amzal, P. A. Butler, K. J. Chan, P. T. Greenlees, G. D. Jones, S. Asztalos, R. M. Clark, M. A. Deleplanke, R. M. Diamond, P. Fallon, I. Y. Lee, A. O. Macchiavelli, R. W. MacLeod, F. S. Stephens, P. Jones, R. Julin, R. Broda, B. Fornal, J. F. Smith, T. Lauritsen, P. Bhattacharyya, and C. T. Zhang, Nucl. Phys. **A645**, 61 (1999).

[23] M. Gai, J. F. Ennis, D. A. Bromley, H. Emling, F. Azgui, E. Grosse, H. J. Wollerheim, C. Mittag, and F. Riess, Phys. Lett. **A215**, 242 (1988).

[24] A. Arima and F. Iachello, Ann. Phys. (NY) **99**, 253 (1976).

[25] G. A. Leander, W. Nazarewicz, G. F. Bertsch, and J. Dudek, Nucl. Phys. **A453**, 58 (1986).

[26] L. Grodzins, Phys. Lett. **2**, 88 (1962).

[27] P. A. Butler and W. Nazarewicz, Nucl. Phys. **A533**, 249 (1991).

[28] W. Nazarewicz, G. A. Leander, and J. Dudek, Nucl. Phys. **A467**, 437 (1987).

[29] M. E. Debray, M. A. Cardona, D. Hojman, A. J. Kreiner, M. Davidson, J. Davidson, H. Somacal, G. Levinton, D. R. Napoli, S. Lenzi, G. deAngelis, M. DePoli, A. Gadea, D. Bazzacco, C. Rossi-Alvarez, and N. Medina, Phys. Rev. C **62**, 024304 (2000).